Journal Pre-proof

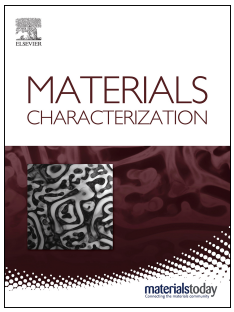

Reobservations of ferrite recrystallization in a cold-rolled ordered Fe–50Co–10V alloy using the EBSD method

Mohammad R. Kamali, L. Pentti Karjalainen, Ali R. Mashregi, Saeed Hasani, Vahid Javaheri, Jukka Kömi

PII: S1044-5803(19)32077-7

DOI: https://doi.org/10.1016/j.matchar.2019.109962

Reference: MTL 109962

To appear in: *Materials Characterization*

Received Date: 2 August 2019

Revised Date: 10 October 2019

Accepted Date: 10 October 2019

Please cite this article as: M.R. Kamali, L.P. Karjalainen, A.R. Mashregi, S. Hasani, V. Javaheri, J. Kömi, Reobservations of ferrite recrystallization in a cold-rolled ordered Fe–50Co–10V alloy using the EBSD method, *Materials Characterization* (2019), doi: https://doi.org/10.1016/j.matchar.2019.109962.

Reobservations of ferrite recrystallization in a cold-rolled ordered Fe-50Co-10V alloy using the EBSD method

Mohammad R. Kamali[1,2], L. Pentti Karjalainen[1], Ali R. Mashregi[2], Saeed Hasani[2], Vahid Javaheri[1], Jukka Kömi[1]

[1]*Centre for Advanced Steels Research, University of Oulu, P.O. Box 4200, FI-90014 Oulu, Finland*

[2]*Department of Mining and Metallurgical Engineering, Yazd University, Yazd, Iran*

Abstract

Even after extensive research for decades on cold-rolled magnetic Fe-Co-V alloys, many aspects of ferrite recrystallization are still unclear. In order to analyse the progress of recrystallization in an Fe-50Co-10V (in wt.%) alloy, different thermal cycles were conducted for an 86% cold-rolled thin sheet (~140 μm). A comprehensive phase characterization and texture analysis were carried out using X-ray diffraction and scanning electron microscopy. To investigate the ferrite recrystallization during concurrent ordering and austenite transformation processes, the utilization of several methods such as the Kernel Average Misorientation and Grain Orientation Spread analyses together with grain boundary misorientation and grain size distributions, and characterization of microstructure by electron backscatter diffraction were crucial. The austenite transformation, detected to start at 500–550 °C, complicated the determination of the recrystallization kinetics; however, it was clarified by the present multi-parameter analyses. The ferrite recrystallization was found to initiate at 600 °C within 1 hour and progress by the continuous recrystallization mechanism. The typical gamma-fiber texture of the cold-rolled alloy remained almost unchanged upon annealing temperatures up to 750°C, also confirming the continuous recrystallization mechanism, similarly as the grain boundary misorientation evolution did. The recrystallization kinetics was found to follow the Avrami model with constant exponent in both ordered and disordered states. The recrystallization rate was slow, so that even after 4 hours annealing in the disordered state at 750°C, fragments of ferrite grains with straight sub-boundaries were retained.

Keywords: Fe-Co-V alloy; ordering; austenite transformation; recrystallization; electron backscatter diffraction; microstructure characterization

1. Introduction

The magnetic alloys containing iron and 50–52% cobalt with 5–13% vanadium (compositions are in wt.%) were invented as hard magnetic materials more than 50 years ago [1]. The vanadium alloying makes these alloys suitable for applications requiring a high magnetic moment, such in synchronous hysteresis motors [2,3]. In order to reach the desired magnetic properties in manufacturing, a severely cold-rolled thin sheet must be subjected to a heat-treatment, where the optimal parameters depend on the chemical composition of the alloy. Recrystallized fraction, grain size, ordering transformation and boundary spacing have been suggested as variables affecting the compromise of magnetic and mechanical properties of a near equiatomic Fe-Co–2V alloy [4]. There are numerous studies on Fe-Co-2V alloys in particular, and Sourmail [5] and Sundar and Deevi [6] have presented comprehensive reviews about the constitution, processing, microstructure evolution, and mechanical and magnetic properties of Fe-Co and Fe-Co-X alloys. Microstructural evolution and mechanical properties of a 36.5Fe-Co-10.6V alloy were studied by Zel'dovich et al. [7,8] already on 1970's, and recently Hasani et al. [9–11] investigated numerous aspects of a 43.25Fe-Co-7.15V alloy.

The softening of cold-rolled structures of these alloys during thermal treatment is a complex phenomenon consisting of several different processes such as order-disorder transition, austenite polymorphic transformation and recrystallization of the ferritic matrix, which all can take place even simultaneously but with the different kinetics during heating and annealing [12]. Interaction of these concurrent processes complicates the situation, and for instance, recrystallization can be retarded by the ordering due to reduction of dislocation movement and grain boundary mobility [5,13]. The distinction between microstructural evolution due to recrystallization and phase transformation is not straightforward. Therefore, still there is some lack of knowledge on the progress of the above processes and microstructure evolution in the Fe-Co based alloys.

In equiatomic Fe-Co alloy the ordering rate is very fast [14]. According to Zakharov et al. [1], the existence of ordering was testified by neutron diffraction for the alloy containing 10.5% V (Vicalloy-1) by Zel'dovich et al. [7,8]. Hasani et al. [15] reported that in an Fe-Co-7.15V alloy the ordering occurs during annealing below 500 °C at a moderate rate and between 500 and 725 °C the alloy orders rapidly.

In addition to ordering transformation, fcc-austenite phase (paramagnetic precipitates) can form from the bcc-ferrite during the treatment [16]. Zakharov et al. [1] claimed that in the alloy containing 7%V, the temperature interval of the ferrite to austenite transformation is located above the optimal annealing temperature (620 °C). However, Hasani et al. [11] reported the start of austenite transformation at 490 °C for a Fe-Co-7.15V (at a heating rate of 10 °C/min) using the dilatometric results. Anyhow, the temperature intervals of the ordering and ferrite-austenite transformations overlap for Fe-Co-10.5%V [1,7,8].

Many researches have investigated the recrystallization of Fe-Co alloys in order to increase the coercive force through the grain refinement [17–20]. However, distinct inconsistences exist regarding the occurrence of static recrystallization, especially in 7–

13%V alloys, where the temperature ranges of the ordering and austenite transformation overlap with that of recrystallization. Recrystallization is considerably retarded by previous ordering of the deformed matrix [5,6,21]. This effect is attributed to a reduction in the mobility of the interface between the growing recrystallized grain and the deformed matrix when both are ordered [5]. Buckley investigated the recrystallization in Fe-50Co-0.4Cr alloy [22] as well as Fe-Co-2.5V alloy [23]. For the former, four temperature ranges were determined. In the temperature range of 250 to 475 °C, recrystallization took place by the nucleation and growth of very fine ordered recrystallized grains within the disordered deformed matrix. Due to the rapid ordering at higher temperatures, recrystallization did not occur at all in the temperature range of 475 to 600 °C, whereas recovery and recrystallization proceeded slowly between 600–730 °C. Finally, at temperatures above 730 °C in the disordered state, recrystallization became increasingly rapid. However, for the alloy containing vanadium, recrystallization was not observed below the critical temperature of the ordering transformation, $T_C \approx 730$ °C. The influence of the ordered state was also reported by Hasani et al. [19] and Nabi et al. [20], pointing out the occurrence of partial recrystallization in Fe-Co-V alloys at temperatures below T_C. In contrast, Duckham et al. [24] reported that recrystallization was almost completed after 1 hour at 600 °C for a cold-rolled Fe-Co-1.8V-0.3Nb alloy and Mao et al. [21] showed that the recrystallization can readily take place at temperatures above 600 ºC in cold-worked Fe-Co.

Thus, even though the Fe-Co-V alloys have been investigated for several decades, recrystallization phenomenon is one of the issues which have not been firmly established and understood yet. Accordingly, in the present work, the softening behavior of a heavily cold-rolled Fe-Co-10V alloy has been studied by comprehensive examinations of microstructural and texture evolution utilizing X-ray diffraction and electron backscatter diffraction (EBSD). In addition to that, the simultaneous ordering and austenite transformation processes have been investigated in detail and mechanical and magnetic properties have been measured, but these results will be reported separately in other papers. Here only the most essential results, which are related with the recrystallization, have been shown.

2. Material and Methods

The experimental raw materials were melted in an electric arc furnace to cast a high purity 50Co-40Fe-10V alloy. For melting, the furnace was evacuated till 10^{-3} mb followed by purging using high purity Ar gas at least for 3 times. At the last stage, Ar was injected into the chamber to supply 500 mb pressure and then electric arcing was initiated. The chemical composition, determined by the inductively coupled plasma mass spectrometry, is given in Table 1. For homogenization, the cast ingots were annealed at 1200 ºC for 10 hours under high purity Ar gas atmosphere followed by quenching in water. After eliminating the surface layer using sand paper grinding, the homogenized ingots were subjected to hot rolling at 850–950 ºC to obtain sheets with the thickness of 1 mm (~ 90% reduction) followed by air cooling to room temperature. Then, severe 86%

cold rolling was performed to prepare strips with the thickness of 140 µm. It is known that the high temperature fcc-phase transforms into a bcc-phase upon air cooling in alloys containing 10–13% V [25]. After the cold rolling process, annealing heat treatments were carried out at a heating rate of 5 °C/s up to different temperatures for various durations. Finally, pieces of thin strips were cooled to room temperature inside the tube furnace at a rate of 10 °C/s via high purity argon gas.

For the phase determination, a Rigaku Smart Lab 9 kW X-ray diffractometer with a Co rotating anode operated at 40 kV and 135 mA in the back-reflection mode and a step size of 0.02° was employed.

Table 1. Chemical composition of the studied alloy.

Element	Co	Fe	V	Cr	Mn	Zn	C	P	S
Amount (wt.%)	49.8	40.1	9.96	0.06	0.009	0.002	0.002	0.01	0.001

Sample preparation for EBSD analysis were performed through the mechanical polishing finalized by 0.25 µm diamond past. Deep etching for SEM imaging was done using a 2.5% $FeCl_3$ solution and duration around 25 s at room temperature. Microstructural investigations as well as micro-texture analysis were carried out using a Zeiss Sigma field emission scanning electron microscope (FESEM) equipped with an EBSD detector. EBSD mappings were recorded using an accelerating voltage of 15 kV, a working distance of 15 mm, a tilt angle of 70° and step size of 30 nm. EBSD post-processing and analyses were performed using the EDAX-OIM analysis software.

3. Results and Discussion

3.1 Ordering process

XRD patterns of some cold-rolled and annealed samples are displayed in Fig. 1. For better clarification, only the 2θ degrees higher than 55º are presented here. Chon et al. [26] reported that the superlattice diffraction peaks due to the ordering in the ferrite phase are visible at 2θ = 36.5º and 65.7º associated with (100) and (111) planes, respectively. Consistently with this, the XRD patterns revealed a superlattice reflection at 2θ ≈ 65.5º after annealing at temperatures of 500–700 ºC for 2 hours. The start of the ordering was also observed in dilatometric curves above 320 °C (not shown here). The height of the peak related to the ordered phase increased from 400 to 600 ºC and then decreased so that no superlattice reflection existed after annealing at 750 ºC. The results show that the cold-rolled bcc martensite was disordered but it became ordered above 400 °C, and the order-disorder transformation occurs between 700 and 750 ºC. The latter range is identical to that of the binary 50Fe-50Co alloy [6]. Sourmail [5] refers to the literature where the ordering temperature of Tc = 732 °C has been reported for the

equiatomic Fe-Co, although values as low as 710 °C have also been given. Nabi et al. [20] reported Tc ≈ 720 °C for an Fe-Co-2V alloy. It means that vanadium addition does not change the critical temperature of ordering transformation significantly. According to Hasani et al. [11], the ordered phase is present in the specimens annealed between 400 and 750 °C, so that the maximum degree of order in an Fe-Co-7.15V is achieved by annealing at 600 °C. The ordering kinetics and mechanism have been discussed extensively in Sourmail's review [5].

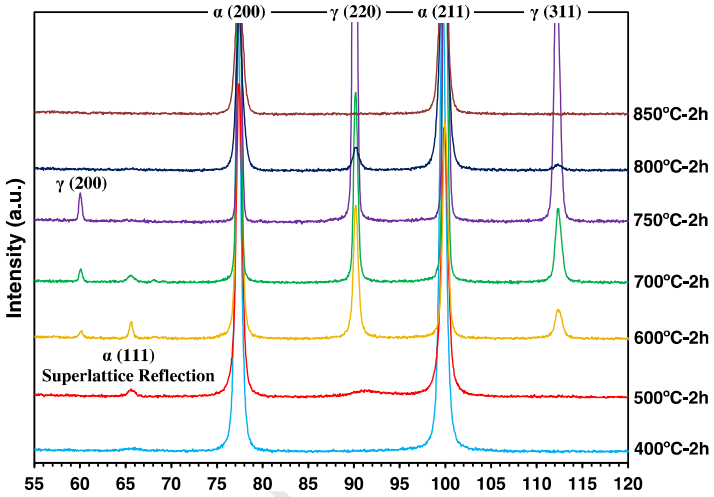

Fig. 1. X-ray diffraction patterns of samples heat treated at various temperatures for 2 hours.

3.2 Austenite transformation process

The polymorphic austenite transformation will be described in more detail in a future paper. However, because it interferes with recrystallization and highly complicates the interpretation of experimental results concerning recrystallization kinetics, some observations are reported here. As seen in Fig. 1, the austenite (220) peak appear in the X-ray patterns in a sample heat treated at 500 °C. The intensities of the austenite peaks increase with increasing the annealing temperature and reach the maximum at 750 ºC. At 800 °C, the austenite diffraction peaks are small and only the ferrite reflections remain after annealing at 850 °C. These XRD results (together with the dilatometry, not shown here) suggest that the two-phase region lies in the temperature range ≈ 500–840 ºC. Above that, a single-phase austenite phase exists but this austenite transforms to martensite during cooling. The martensite start temperature M_S was 280 °C in the dilatometric curve (at the cooling rate of 10 °C/min). Thus, in the present instance, the temperature intervals of the ordering and austenite transformations overlap at temperatures above 500°C, as also reported by Zel'dovich et al. [7,8] for an Fe-Co alloy with 10.5V.

Comparing the observed temperature range with the two-phase region ~ 935–955 ºC of the binary 40Fe-60Co alloy [27], and 760–900 °C for an Fe-52Co-7V alloy [1], it is obvious that the vanadium addition decreases drastically the start temperature of the

allotropic transformation and extends the width of the two-phase region. This is seen from the plot of the phase boundaries in Fig. 2, as quoted and modified from the review of Sourmail (see Fig. 4 in Ref. [5]). Hasani et al. [11] reported a temperature as low as 490 °C (heating at 10 °C/min) for the start of the contraction in a dilatometric curve and found an austenite XRD peak after annealing at 600 °C for an Fe-Co-7V alloy.

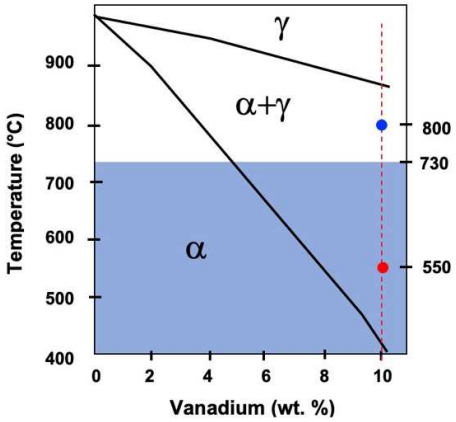

Fig. 2. The two-phase region in V-bearing equiatomic Fe-Co alloys, as modified from Ref. [5]**. The ordering region is highlighted in blue color. Samples annealed for 2 hours at 550 and 800 °C containing ferrite and austenite phases, detected using EBSD, are shown by dots.**

The formation of small particles could be detected by FESEM and EBSD phase map. Fig. 3 presents secondary electron micrographs of heavily etched samples after annealing for 2 hours at 550 °C (Fig. 3(a)) and 650 °C (Fig. 3(b)). It was seen that new tiny grains begin to precipitate along ferrite grain boundaries. These grains seem to occupy wider zones at higher temperatures and particles coalescence together.

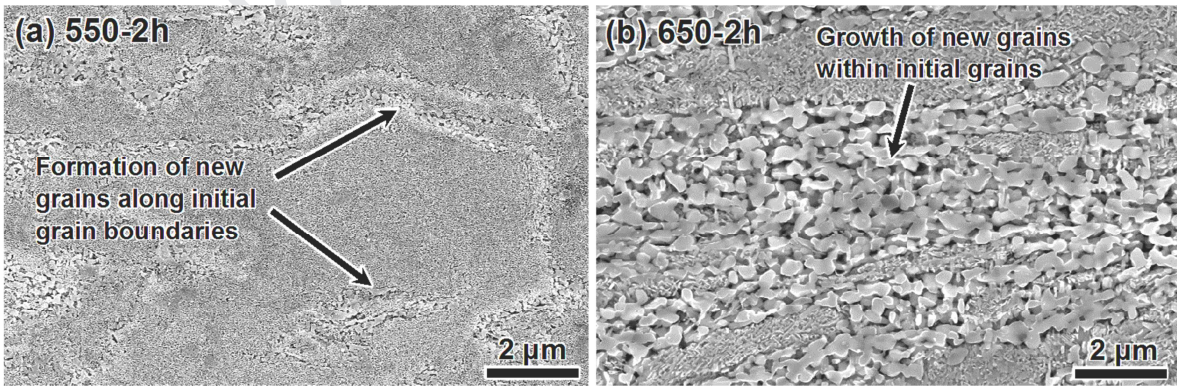

Fig. 3. New grains forming on ferrite grain boundaries in cold-rolled samples heat treated at (a) 550 °C for 2 hours and (b) 650 °C for 2 hours. SEM secondary images of heavily etched samples.

The features, resembling those in Fig. 3, have been reported as recrystallization of ferrite in some investigations [15,24,28]. However, extensive EBSD examinations revealed contradictory results. According to the phase maps shown in Fig. 4, many new grains along ferrite grain boundaries are not ferrite but austenite. First austenite particles were detectable at 550 °C after 2 hours (Fig. 4(a)), and the fraction of austenite increased with increasing annealing temperature, depicted in Fig. 4(b) (650 °C for 2 hours). This

austenite is thermally stable and retains during cooling to room temperature. The observations are consistent with the XRD analysis which showed the presence of austenite phase at and above 500 ºC. The austenite transformation in Fe-Co alloys is well reported in the literature [5–7] and some authors distinguish between low- and high-temperature austenite [29]. Details on phase and microstructural analysis will be discussed in a future paper.

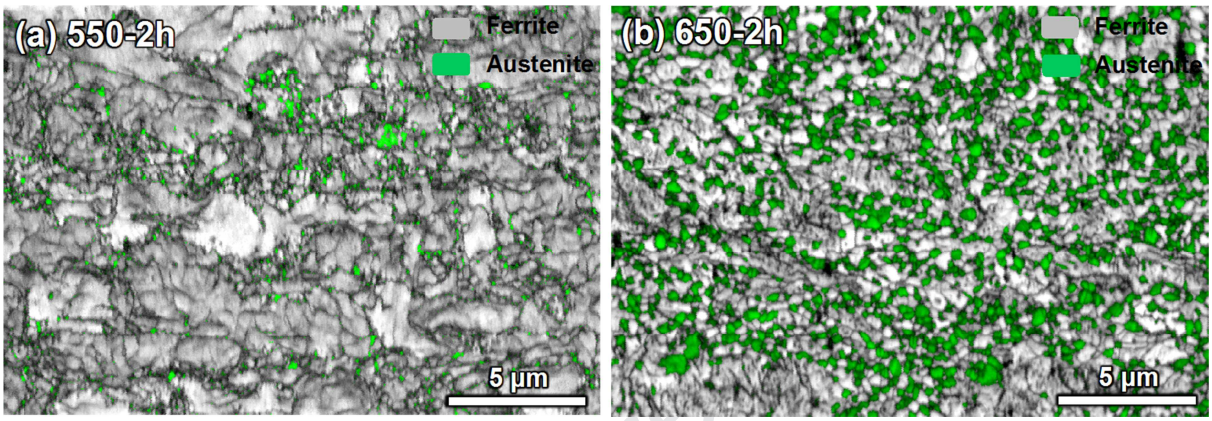

Fig. 4. Austenite transformation in cold rolled samples annealed for 2 hours at (a) 550 ºC and (b) 650 ºC. EBSD image quality and phase maps.

With increasing the annealing temperature, the fraction of austenite measured by EBSD at room temperature increased up to 750 ºC (63% austenite after 2 hours holding; see later Fig. 11(c)) but decreased then. This is because some of the austenite transformed back to the bcc-phase during cooling from 750 °C and above, so that only a fraction of austenite formed at high temperature was retained. In agreement, the XRD patterns in Fig. 1 showed decreased austenite reflections at 800 °C and no austenite peaks after cooling from 850 °C.

3.3 Recrystallization process

As mentioned earlier, there are inconsistent reports concerning the recrystallization in Fe-Co based alloys owing to the complex interference of different phenomena, which are taking place concurrently during heat treatment, as discussed by Sourmail [5]. In the present study, the EBSD technique was employed extensively to examine the various features of the recovery and recrystallization of the ferrite phase. The progress of recrystallization was followed by the Kernel Average Misorientation (KAM) and Grain Orientation Spread (GOS) techniques, and the microstructure evolution was characterized by image quality (IQ) and phase maps together with grain boundary misorientation and grain size distributions. Finally, the recrystallization mechanism was determined from EBSD IQ and grain boundary maps and further confirmed by the texture characterization.

3.3.1 Recrystallization kinetics

3.3.1.1 KAM analysis

The KAM data represents the average misorientation angle of a given point with respect to all its neighbors. The KAM can be used to describe local dislocation density distribution and the recrystallization fraction [30]. In a recrystallized material it is expected that the KAM values can approach to zero because new grains which form during recrystallization are defect-free grains [31]. In this regard, the absolute misorientation value of 0.5º was found optimal as a criterion for distinguishing dislocation-free regions in the matrix, even though also the value of 1° has been used for that, e.g. in Ref. [30].

Fig. 5 displays the KAM maps of samples annealed at various temperatures for 2 hours. The maps reveal areas with high dislocation density (KAM value ≥0.5°) as green region and low strain areas as blue one (KAM <0.5°). It is seen that the high-strain area fraction decreases significantly from 76% for a sample annealed at 500 °C to 50% while annealed at 600 °C. However, the high-strain KAM area fraction is still 18% even after annealing at 750 °C for 2 hours, which suggests that the recrystallization is not completed even then. In the simplest instance, the decrease of the high-strain area would correspond to a fraction of recrystallized ferrite, but as noted, also the austenite transformation takes place simultaneously with recrystallization, so that low KAM values also include strain-free austenite in addition to recrystallized ferrite. However, even more, we have to realize that the low-strain area fraction is much higher than the fraction of austenite and recrystallized ferrite especially after low temperature annealing. The treatment at 550 °C for 2 hours results to the start of austenite transformation (Fig. 4(a)) and there is no recrystallization of ferrite yet (see Sections 3.3.1.2 and 3.3.1.3), so the fraction of 24% of low-strain area must correspond to some local ferrite grains encountered intense recovery (large blue area in Fig. 5(a) as an example). Thus, the KAM analysis seems to be an ineffective method to characterize the recrystallization of ferrite in the present alloy.

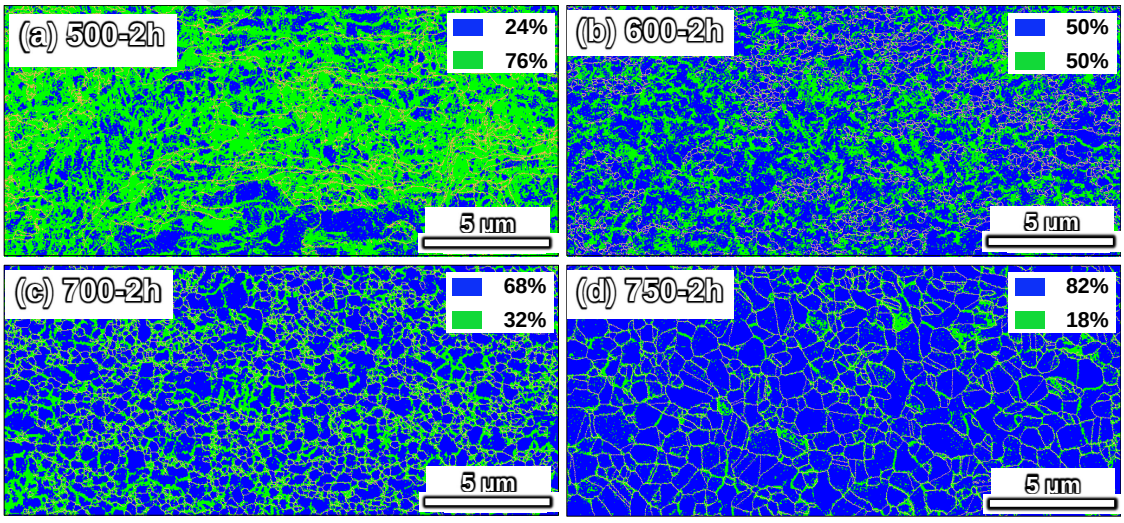

Fig. 5. KAM maps for samples annealed at various temperatures showing high-strain (green) and low-strain (blue) areas. The fractions are given in the images.

3.3.1.2 GOS analysis

The GOS analysis was also used to follow the progress of recrystallization under various heat treatment conditions. Principles of this method are based on a hypothesis of strain assisted internal rotations of micro volumes like cells or sub-grains within the grains. Deformation of a material leads to distortion of grains, which results in a high GOS value while recrystallized (deformation-free) grains possess a low GOS value close to zero [32]. Thus, similarly to KAM, GOS is a parameter that in principle can distinguish the recrystallized grains from the deformed ones. The threshold value for GOS varies between 1 and 2° in various studies, e.g. [33,34]. To determine the optimal threshold limit, the GOS value distribution obtained in some present experiments has been plotted in Fig. 6(a). It is seen that the change is abrupt at 1°, so the threshold limit of 1° was selected as a criterion for quantification of recrystallization.

Similarly as for KAM, owing to the concurrent occurrence of recrystallization and austenite transformation, which both processes lead to strain-free grains, measurement of the exact fraction of recrystallized ferrite seems complicated. However, it is possible to subtract the data of the fcc-phase using the OIM software and apply the GOS analysis only to the bcc-phase, and this was considered as a useful approach for estimating the recrystallization fraction. Still a concern in this situation is whether any recrystallized ferrite grains transform to austenite during prolonged heating and retain to room temperature, consuming thereby recrystallized ferrite grains. Without knowing how this is, it was assumed that the preferred grains for transforming to austenite are non-recrystallized ferrite grains, which have a higher number of nucleation sites for austenite nucleation. Moreover, strain energy in deformed grains reduces the nucleation energy barrier introduced by the formation of austenite-ferrite interfaces, as pointed out by Peranio et al. [35]. Hence, it was considered reasonable to subtract all austenite grains off and analyze the GOS of the ferrite grains only.

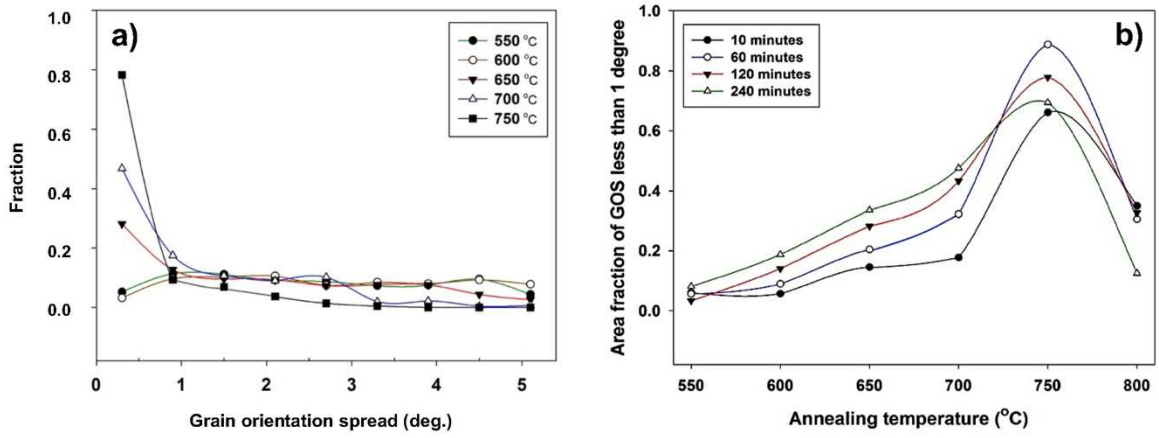

Fig. 6. (a) Grain Orientation Spread distribution curves for samples annealed at various temperatures for 2 hours, (b) fraction of areas with GOS less than 1° for various annealing conditions.

Fig. 6(b) depicts the fraction of GOS values < 1°, i.e., recrystallized ferrite grains in samples heat treated under various conditions. The data are also listed in Table 1. Based

on this figure, it seems that recrystallization starts around 600 ºC within 1 hour and reaches the maximum fraction around 89% after 1 hour at 750 ºC. However, it is seen that there is a base level in the GOS values in Fig. 6(b), which obviously cannot be related to the recrystallized fraction. From the data in Table 2 it can be realized that the GOS values at 500 and 550 °C are independent of the holding time, so this amount, around 6%, is possibly related to the recovery. After subtracting 6% from the values in Table 2, it can be concluded that the recrystallization had hardly initiated at 550 °C but it proceeded at 600 °C.

To make the information of the data clearer, the GOS fractions (after subtracting 6%) vs time curves are plotted in Fig. 7. The sigmoidal type of the curves, typical to the static recrystallization [36], are recognizable in spite of the scarce data. The kinetics is dependent on the annealing temperature (times for the predicted 50% recrystallization are given in Table 3) and the Avrami exponent is constant 0.4. This value is very low revealing a significant influence of recovery, for Huang et al. [37] reported the exponent of 1 for ferrite recrystallization without influence of the recovery. However, from the experimental data it is seen that the maximum fraction of recrystallization within 4 hours remains below 50% (~42%) while annealed at 700 ºC. Increasing the annealing temperature to 750 °C seems to lead to drastic increase in the recrystallization rate and the recrystallized fraction is 60% (6% subtracted) already within 10 min, which still increases during 1 hour up to 83%. This can be attributed to the order-disorder transition in this temperature interval indicating the retarding influence of the ordered state.

Table 2. Area fraction (%) of GOS<1° after various annealing conditions.

Annealing time (min)	Annealing temperature (°C)					
	500	550	600	650	700	750
10	3.2	5.6	6.0	14.5	17.6	66.1
30	3.8	4.6	8.7	16.1	27.3	81.6
60	4.4	5.5	8.9	20.4	32.2	88.7
120	3.1	3.3	14.0	28.1	43.2	77.8
240	4.8	8.1	18.7	33.6	47.5	69.3

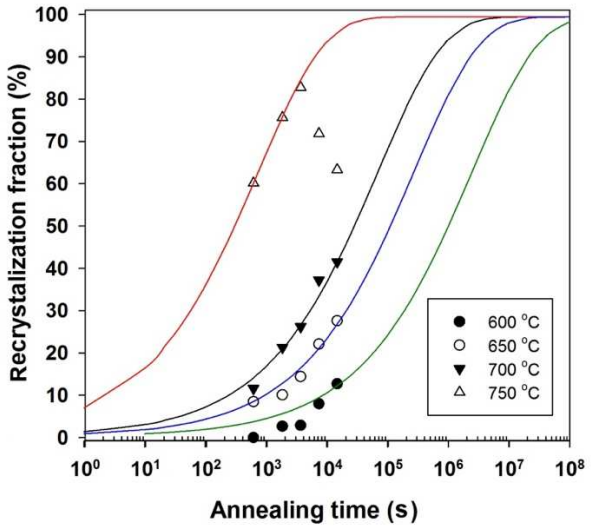

Fig. 7. Recrystallized ferrite fraction after various heat treatments based on GOS analysis (data in Table 1; 6% subtracted as background).

Table 3. Time for 50% recrystallization based on sigmoidal equations fitted with the GOS data (6% subtracted).

T(°C)	t_{50} (s)
600	500000
650	110000
700	28000
750	300

All the estimated recrystallized fractions from the GOS values remain much below the complete recrystallization. A prediction using the sigmoidal equation for the recrystallization fraction at 750 °C suggests that the degree of 97% recrystallization would be achieved within 5 hours and 99% in 10 hours. Furthermore, from the measured values in Table 2, it is seen that the GOS value decreases at longer durations than 1 hour at 750 °C (see also Fig. 6(b)). The fall can be explained as a result from the high-temperature austenite having lower thermal stability (due to lower Co and V contents, to be discussed in a future paper), so that the austenite to martensite transformation has taken place during cooling. Owing to the shear mechanism of martensitic transformation, the GOS value increases with increasing dislocation-rich martensite. Therefore, the real recrystallized fraction of ferrite cannot be read from GOS values for these conditions (durations longer than 1 hour at 750 °C).

3.3.1.3 Grain boundary analysis

Grain boundary misorientation distribution was determined after various heat treatments and these curves for ferrite are plotted in Fig. 8. The deformed and recovered

ferrite contains high number of low angle grain boundaries (LAGBs), and their number is expected to decrease with increasing recrystallization fraction. As expected, the LAGBs (2°–15°) are dominant after low temperature annealing at 400–600 °C. However, with increasing the annealing temperature from 600 °C up to 800 °C, the fraction of LAGBs decreases obviously as a sign of the progress of ferrite recrystallization. The maximum at 45° corresponding to the distribution of boundaries of randomly oriented ferrite grains does not appear [38,39], but the misorientation is quite homogeneously distributed. A small peak at 30° may be an erroneous peak, as pointed out by Ryde [39]. After annealing at 800 °C, a peak appears at 52–59° misorientations, revealing that the bcc-phase is not only ferrite, but also includes martensite. Consistently, Hannula et al. [40] found the misorientation maxima at 52.5° and 59° corresponding to packet or/and block boundaries of martensite in a low carbon steel.

Hasani et al. [15] investigated the misorientation distribution of grain boundaries and fraction of high angle grain boundaries (HAGBs) after various heat treatments in an Fe-Co-7V alloy. They also observed the dominance of LAGBs in cold rolled and at low temperature annealed samples. The fraction of LAGBs decreased with increasing annealing temperature. A misorientation peak at 55° appeared after annealing at 850 °C, obviously as a result of martensitic microstructure, although the reason not pointed out in the work.

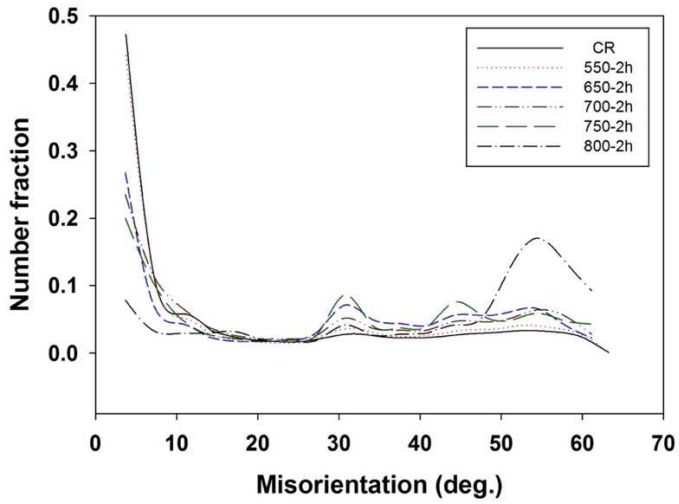

Fig. 8. Grain boundary misorientation distribution for the bcc-phase in samples after various annealing conditions. CR= cold rolled.

As recrystallized grains are surrounded by HAGBs, we can assume that the change in the fraction of HAGBs is a measure of progress and kinetics of recrystallization. In Fig. 9, the fraction of HAGBs is plotted as a function of annealing temperature (Fig. 9(a)) and time (Fig. 9(b)). To exclude the influence of the austenite transformation, which also increases the number of HAGBs, both austenite and austenite/ferrite boundaries were subtracted from the data. From Fig. 9(a), it is obvious that the fraction of HAGBs of ferrite/ferrite-interfaces starts to increase in annealing at 600 ºC and the slope of the curves increases steeply above 700°C. In fact, this is due to the data at 750 °C, i.e.

annealing in the disordered region. In Fig. 9(b), it is observed that the fraction of HAGBs increases with increasing short soaking time, especially at lower annealing temperatures, but soon it reaches practically a saturation level. This seems to suggest that the recrystallization proceeds with time at low temperatures of 600–700 °C but ceases soon. Further, the saturation level depends on the annealing temperature and is distinctly higher for 750 °C than for the lower temperatures, suggesting a microstructure difference in the disordered region compared to that in the ordered region. This could be related to the increased recrystallization rate as observed in Fig. 7. Anyhow, it is obvious that the fraction of HAGBs would never reach 100% at these temperatures, in qualitative agreement with a conclusion drawn from the GOS analysis and microstructural observations, to be shown in Section 1.3.1.4, that the recrystallization remained incomplete under the studied conditions.

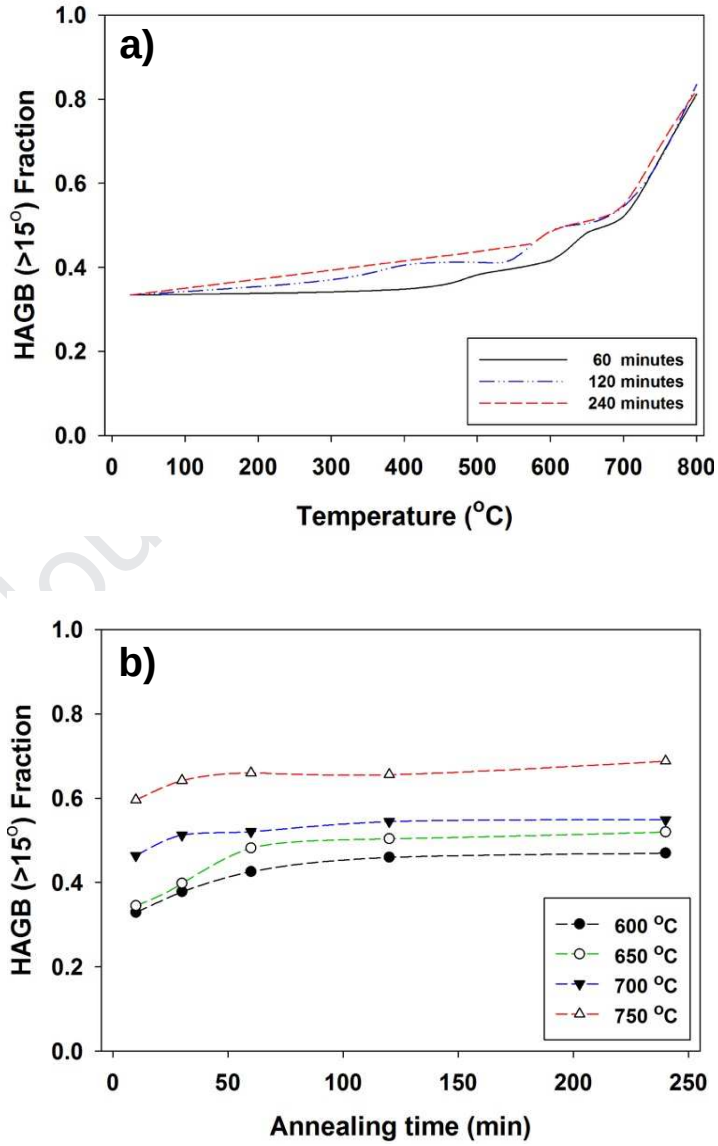

Fig. 9. Fraction of high angle grain boundaries (HAGB) calculated from EBSD data as a function of (a) annealing temperature and (b) annealing time.

Unfortunately, from HAGB fractions we cannot be absolutely certain about the maximum recrystallized fraction of ferrite, because the unstable austenite transforms to bcc-martensite, containing both LAGB and HAGBs and becomes considered as ferrite. Also, the austenite fraction via the number of austenite/ferrite interfaces, which was subtracted, may affect the HAGB value. Thus, it can be concluded that the HAGBs fraction is not an effective measure of ferrite recrystallization in this alloy. Ferrite grains must be examined directly in order to detect whether non-recrystallized grains still exist after annealing but exclude the new martensite grains also having the bcc structure. This issue will be discussed in the following.

3.3.1.4 Microstructure characterization

The EBSD technique was employed to examine the microstructure of the alloy after various heat treatments. Especially the start of recrystallization, the influence of the order-disorder transition on recrystallized microstructure and the maximum recrystallized fraction were of main interests. Fig. 10 depicts a phase map (ferrite gray, austenite green) with blue HAGBs for a sample annealed for 1 hour at 600 °C. Fig. 4(a) shown earlier indicated that only recovered large ferrite grains are visible with few tiny austenite grains after annealing at 550 °C. However, Fig. 10 reveals that at 600 °C within 1 hour, in addition to large ferrite grains few small ferrite grains with irregular shape (shown by arrows), surrounded by HABG, are also formed together with small austenite grains (fcc-phase in green color). Thus, this confirms unambiguously that the recrystallization has initiated, the fraction estimated as 3% by the GOS analysis (Table 2; background subtracted). Without the phase distinction, it would be quite impossible to distinguish these small grains because of simultaneous austenite transformation. Typical to these grains is that they are not equiaxed, but their boundaries are very curved, as shown by the enlarged images in Fig. 10.

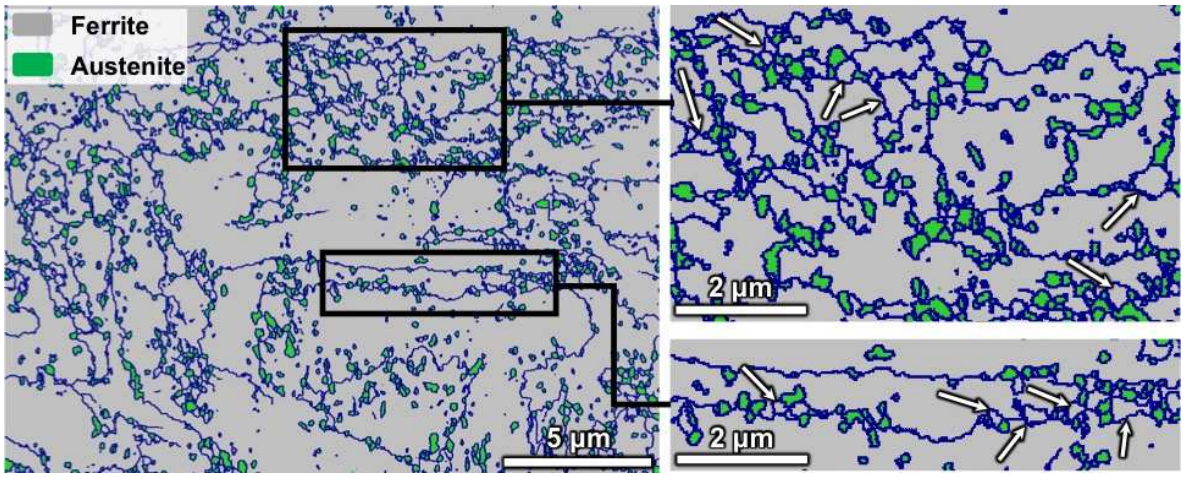

Fig. 10. Start of recrystallization of ferrite and austenite transformation during annealing at 600 °C for 1 hour. EBSD phase map (ferrite gray, austenite green) with HAGBs in black color. Some recrystallized grains are shown by arrows in enlarged images.

Further progress of recrystallization and austenite transformation is seen in Fig. 11, where microstructures after heat treatments at 600, 700 and 750 °C for 2 hours. At 700 °C, the recrystallization fraction is expected to be higher (37% in Table 2), but also austenite fraction has increased. Still the number of LAGBs (red lines) is high at 700 °C and even at 750 °C as a sign of the presence of recovered grains.

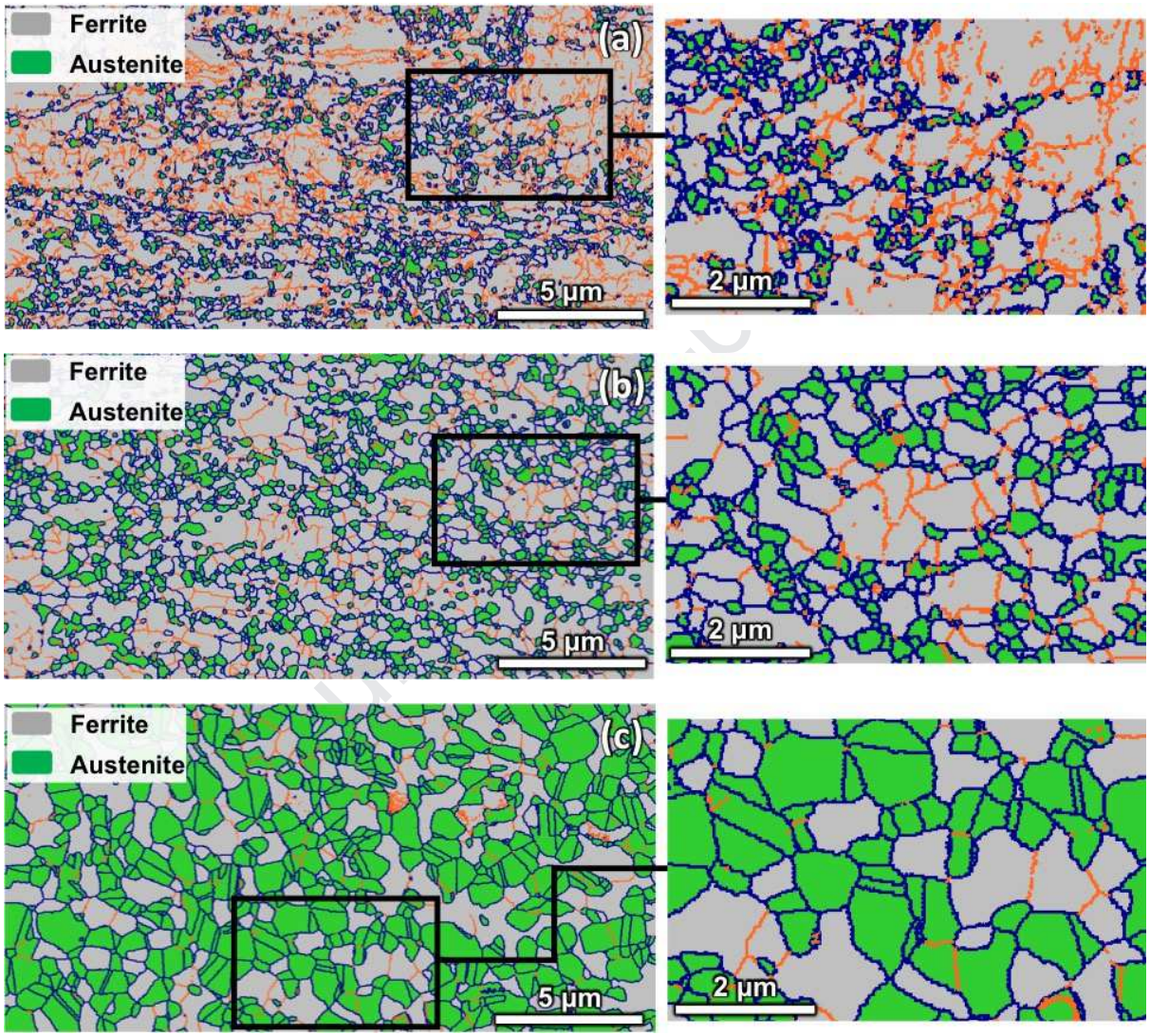

Fig. 11. Recrystallization and transformation of austenite during annealing for 2 hours at (a) 600 °C, (b) 700°C and (c) 750 °C. EBSD grain boundary and phase maps. HAGBs are blue, LAGBs red, ferrite grey and austenite green.

The microstructure after 4 hours annealing at 750 °C is displayed in Fig. 12 as a phase map showing HAGBs (Fig. 12(a)), and overlapped image quality (IQ)-grain boundary-phase maps (Fig. 12(b)). Fig. 12(a) reveals that the fcc-austenite is a major phase with equiaxed grains containing twins (green phase) and the bcc-phase consists of irregular multi-corner grains (gray phase). All ferrite grains may seem recrystallized. However, a careful look at bcc-grains in (a) and (b) reveals that some of them are light (almost white in (b)), whereas some ferrite grains are darker. The difference in IQ means a higher

density of dislocations in darker regions [39,41], so that the darker grains are martensite, not ferrite. From decreasing GOS values in Table 2 after annealing at 750 °C for longer durations, it could be concluded that some austenite grains became unstable and transformed to martensite upon cooling. In addition, sub-boundaries can be observed in some ferrite grains indicating that they are not recrystallized yet. Thus, there exist austenite, martensite, recrystallized ferrite and few non-equiaxed relatively large grains, remnant of original ferrite grains, containing sub-boundaries even after 4 hours at 750 ºC. Consequently, it can be concluded that recrystallization of ferrite would hardly be completed even at temperatures higher than T_C. The duration of 10 hours was estimated to be needed for that (Fig. 7). Zheng and Raabe [42] have discussed and modelled the concurrent recrystallization of ferrite and austenite transformation in low carbon steels. Without austenite transformation the ferrite recrystallization can be completed, but during annealing at the two-phase temperature region, the recrystallized ferrite fraction can reach a maximum and then decrease during prolonged annealing. Then, a considerable amount of ferrite remains non-recrystallized even after a long duration of annealing.

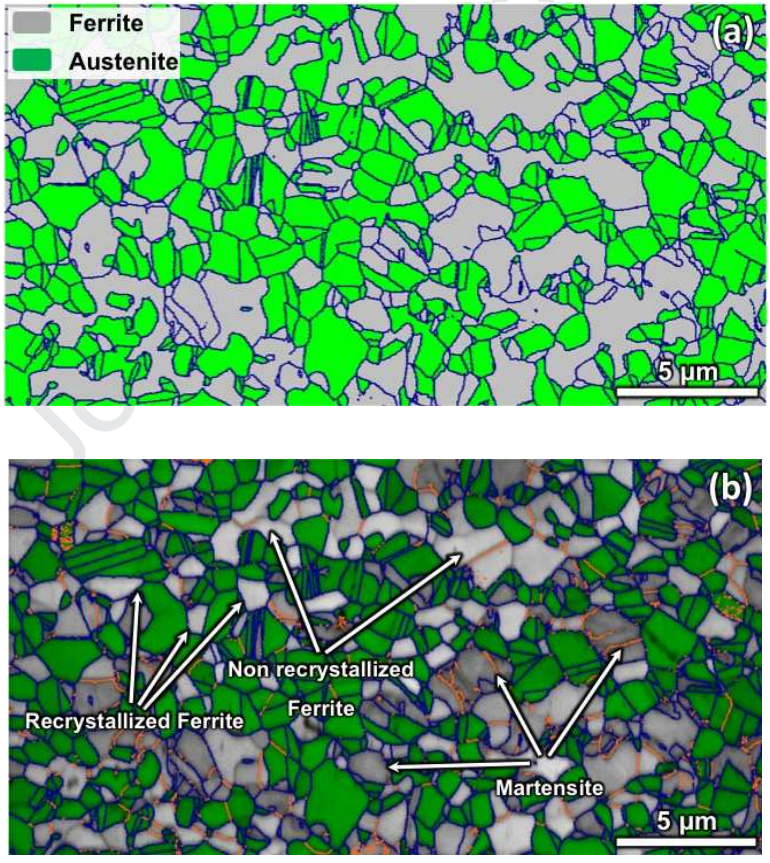

Fig. 12. Microstructure after 4 hours annealing at 750 ºC showing ferrite, martensite and austenite. (a) Phase map (ferrite gray, austenite green), (b) IQ + grain boundary + phase maps (LAGB red, HAGB blue).

Based on the results, the start of ferrite recrystallization in the ordered state at 600°C, the slow recrystallization rate up to 700 °C, and the faster rate at 750 °C in the disordered

state have now been established. This clarify the prior diverse observations reporting the absence of recrystallization below 730 °C [23], partial recrystallization below 730 °C [19,20] or readily occurring recrystallization at 600 °C and above [21,24]. The slow recrystallization kinetics observed can be suggested to result from the several reasons as follows:

(1) In many instances such as in low-carbon steels, grain boundaries are sites for nucleation of recrystallization and austenite transformation, e.g. [37] Therefore, the fast austenite nucleation on grain boundaries in competition consumes the favorable area for recrystallization. Here, the austenite transformation starts even earlier (at 550 °C) than the recrystallization (Figs. 4 and 10). However, as to be confirmed later and can be concluded from the location of small ferrite grains in Fig. 10, the recrystallization occurs by the continuous mechanism, which has no nucleation stage on an HAGB. However, new grains appear adjacent to HAGBs while an LAGB needs to transform to an HAGB only on one side. Hence, HAGBs are favored sites for recrystallization in the present instance, too.

(2) The extensive nucleation of the fine austenite precipitates will stabilize the deformation structure and thus hinder the ferrite recrystallization [42]. At the moving recrystallized/non-recrystallized ferrite grain boundaries the recrystallization front is suffering pinning due to appearance of the fine austenitic particles, which may slow down the recrystallization rate slightly.

(3) Recrystallization is slow due to the ordered structure of ferrite. For instance, Mao et al. [21] and Buckley [23] showed that the recrystallization kinetics is retarded as a result of the sluggish migration rate of grain boundaries in the ordered matrix.

(4) As the fourth reason, it has been reported that paired dislocations are present not only at temperatures below T_C but also at temperatures above T_C, where only short-range order subsists [43]. Hence, we may assume reasonably that at a temperature slightly higher than T_C (730 ºC), the short-range order still exists and slows down the recrystallization.

Thus, the competition between recrystallization and phase transformation can result in incomplete recrystallization. Another phenomenon, a sluggish recrystallization at the final stage of the process, retaining non-recrystallized grains, has been reported for ferritic stainless steels, e.g. by Mehtonen et al. [44]. This has been explained as a result from heterogeneous sub-grain structure, where largest sub-grains cannot form new sub-grains for nuclei of recrystallization. In fact, huge differences can be seen existing in sub-grain size at 550 °C (Fig. 4(a)) and 600 °C (Fig. 11(a)).

3.3.1.5 Grain size distribution

Fine grain size is desired for high mechanical strength and also for magnetic properties (coercivity), as pointed out by many authors [5,19,20,45]. Formation of fine grains is also an indication of the progress of recrystallization after heavy cold rolling. Fig. 13 shows some plots of ferrite grain size distributions based on EBSD runs. Certain facts can be seen from the curves. The fraction of large initial grains still existing at 550

°C is decreasing gradually revealing that new smaller recrystallized grains have formed at higher annealing temperatures. The area fraction of small grains has increased significantly during annealing at 750 °C showing that the recrystallization was there much faster than at 700 °C. The highest fraction is around 1 µm which means that even submicron grains have formed. After annealing at 800 °C, the grain size is quite homogeneous, and slightly larger than at 750 °C, indicating that some grain growth tends to take place, but the grain size is still fine, order or 1–2 µm.

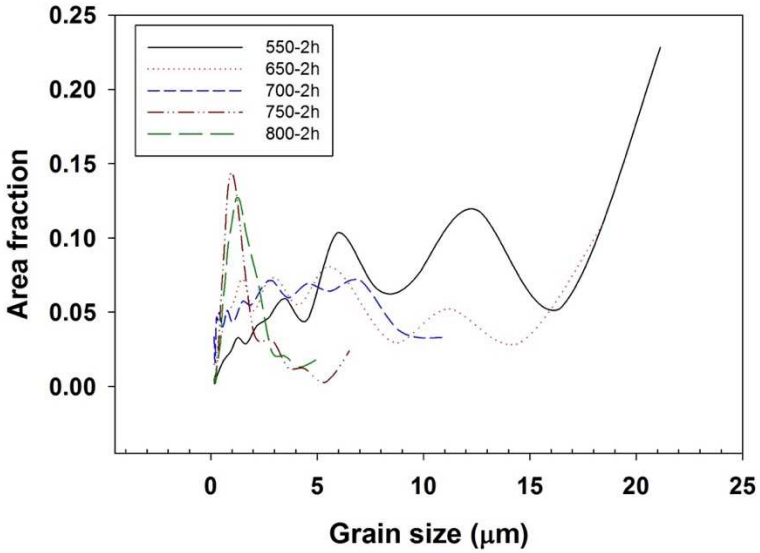

Fig. 13. Grain size distribution of the ferrite after annealing at various temperatures for 2 hours.

According to the grain size data in Sourmail's review [5] (Fig. 36 therein) and research conducted by Ren et al. [46], the recrystallized grain size varied between 4.5 and 16 µm in an Fe-Co-2V-0.5Nb alloy after holding for different times (10 min – 20 h) at 820 °C. Thus, the grain size was much larger than at present. However, grain sizes below 1 µm have been obtained in Fe-Co-V-Ni alloys, held 2 hours at a temperature between 650 and 750 °C [5]. Duckham et al. [24] reported the grain size as fine as 290 nm in an Fe-Co-2V-0.3Nb alloy after annealing at 650 °C for 1 hour. The structure was claimed to be ordered and completely recrystallized based on transmission electron microscopy. The present observations (Figs. 10, 11 and 13) indicate that recrystallization can lead to submicron grain sizes, but the partial recrystallization readily results in wide grain size distribution. The pinning effect of austenite particles on grain boundaries is an obvious factor reducing grain growth.

3.3.2 Recrystallization mechanism

3.3.2.1 Grain structure evolution

The KAM analysis in Fig. 5 showed significant reduction in the high-strain area while annealed at 600 °C compared to the annealing at 500 °C. However, recrystallization seemed to be at a very early stage at 600 °C (8% fraction estimated after 2 hours), so that

the change must be related to the recovery process in the ferrite, i.e. formation of sub-boundaries and annihilation of dislocations. Figs. 10 and 11 revealed LAGBs/sub-boundaries in ferrite and also a high fraction of LAGBs was seen in grain boundary misorientation analysis (Fig. 8). Careful EBSD examinations of the ferrite grain structure showed that LAGBs inside the deformed ferrite grains tended to transform to HAGBs and thereby create new ferrite grains. The growth of the misorientation is evidenced in Fig. 14, where grain boundaries with the misorientation 2–5°, 5–15° and higher than 15° are shown by red, green and blue colors respectively. The presence of these LAGBs and HAGBs firmly show that the active mechanism is the continuous recrystallization, where LAGBs gradually increase their misorientation until HAGBs are formed. The continuous recrystallization has been reported as the recrystallization mechanism in ordered Fe-Co-V alloys also by Mao et al. [21], but they claimed that the recrystallization in the disordered state was based on conventional discontinuous (nucleation and growth) mechanism. However, as seen in Fig. 14, similar evolution of misorientation from 2° to 15° can be seen both at 650 °C (Fig. 14(a)) and 750 °C (Fig. 14(b)), i.e. below and above the T_C of 730 °C. Thus, the continuous recrystallization mechanism seems plausible also in the disordered region.

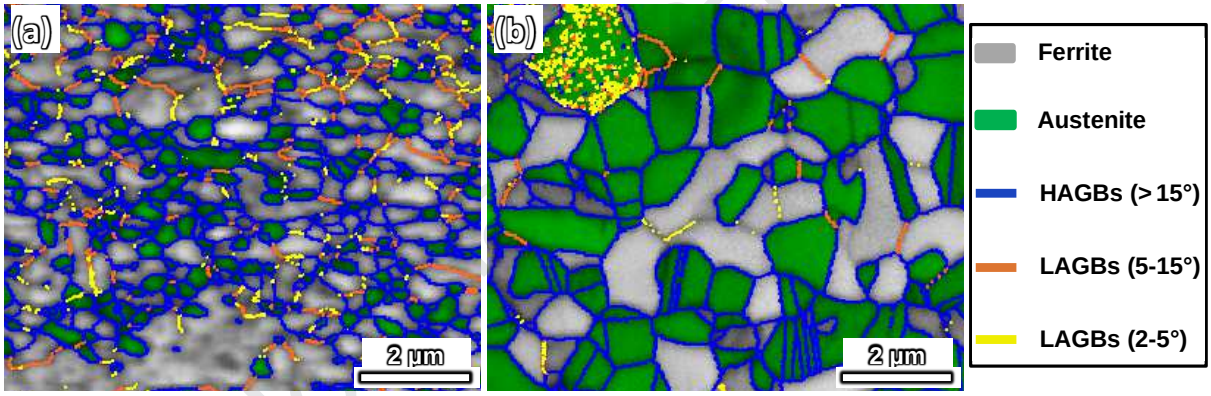

Fig. 14. Ferrite grains with grain boundaries with different misorientation degree as an evidence of continuous recrystallization. (a) 650°C-2h and (b) 750°C-4h.

3.3.2.2 Texture analysis

In order to further confirm the recrystallization mechanism in the present alloy, micro-texture analysis of the ferrite phase was carried out. EBSD measurements were used to calculate the orientation distribution functions (ODF) in the three-dimensional Euler space. In bcc metals like the studied material, the main texture components, in both the deformed and annealed condition, are found in the φ_2= 45° section of the Euler space [47,48]. Fig. 15 shows such ODF maps for the cold-rolled condition and after annealing at different temperatures. The texture of the samples was the typical texture of a bcc material, when formed from deformed austenite, consisting mainly of ND//<111>, i.e. γ-fiber, and RD//<110>, i.e. α-fiber. In addition, the ODF sections show that the texture of the samples is essentially the same for all the conditions almost independently of the annealing temperature. Further details about the texture evolution as function of annealing temperature is presented in Fig. 16. It is observed that the texture is more pronounced along to the γ- and ε-fibers, which are the most important fibers for rolled

samples under plain strain deformation, as well as the rotated cube component. With regard to Figs. 15 and 16, the maximum orientation intensity is observed near the rotated cube $\{001\}\langle 110\rangle_{\alpha}$ and transformed Goss $\{111\}\langle 110\rangle_{\alpha}$ components and the transformed brass and copper along to the ε-fiber. Of course, because of symmetry, there is an intensity peak at the beginning of the ε-fiber corresponding to that at the beginning of the α-fiber.

It should be noted that in the case of the nucleation of the new grains in the course of the recrystallization, the texture, at least the intensity of the texture components, should change with respect to the fraction of recrystallization. However, such the change does not happen in the present instance, so the texture behavior can be considered as a reliable evidence for the occurrence of continuous recrystallization instead of the conventional discontinuous static recrystallization [5,49]. This is in agreement with suggestions of Mao et al. [21] on an Fe-Co alloy.

Contrarily, during recrystallisation in the disordered region, the {111} rolling texture is replaced by a {111} recrystallisation texture according to Mao et al. [21]. However, in the present instance, the texture after annealing at 750 °C is equal to the texture of the cold rolled sheet and to those annealed at lower temperatures, which suggests that the recrystallization mechanism is still continuous recrystallization. The same conclusion is also drawn from the existence of sub-boundaries in ferrite in samples annealed at 750 °C (Fig. 14(b)).

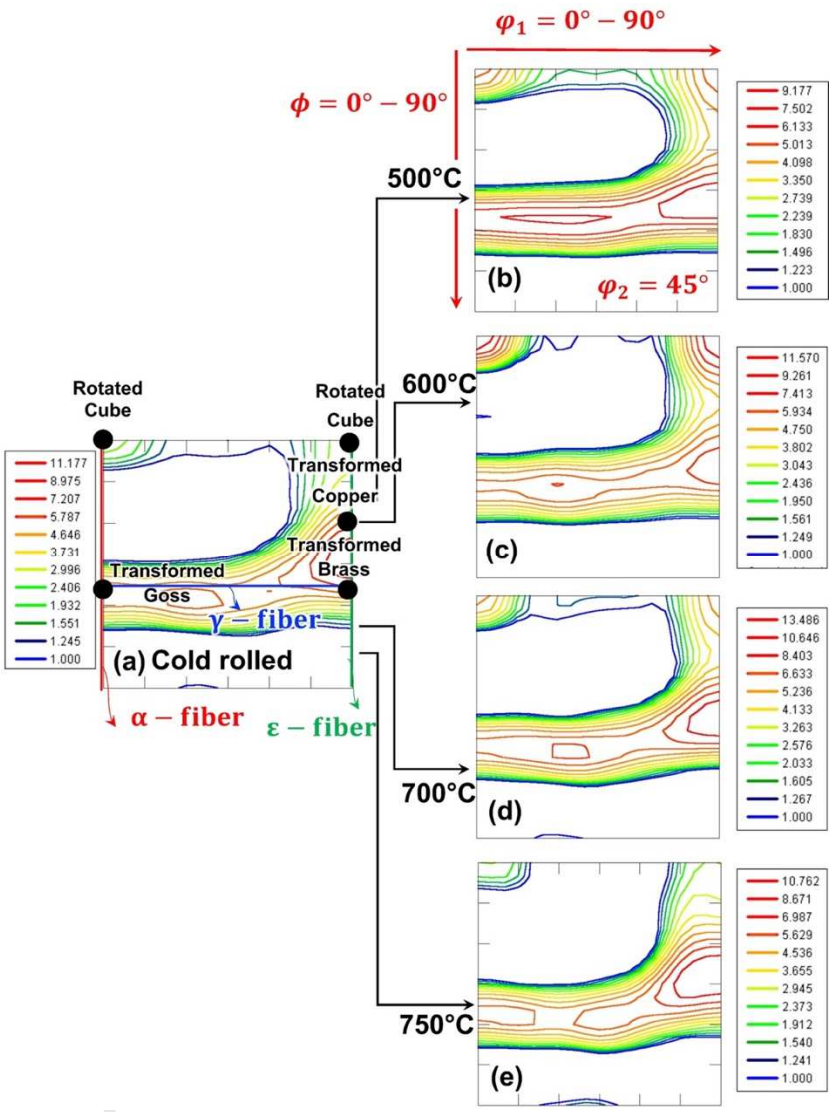

Fig. 15. ODF sections at φ2=45°. a) Cold-rolled, b) 500°C-2h, c) 600°C-2h, d) 700°C-2h and e) 750°C-2h; along with the location α, γ and ε-fibers and some important components in the Euler space.

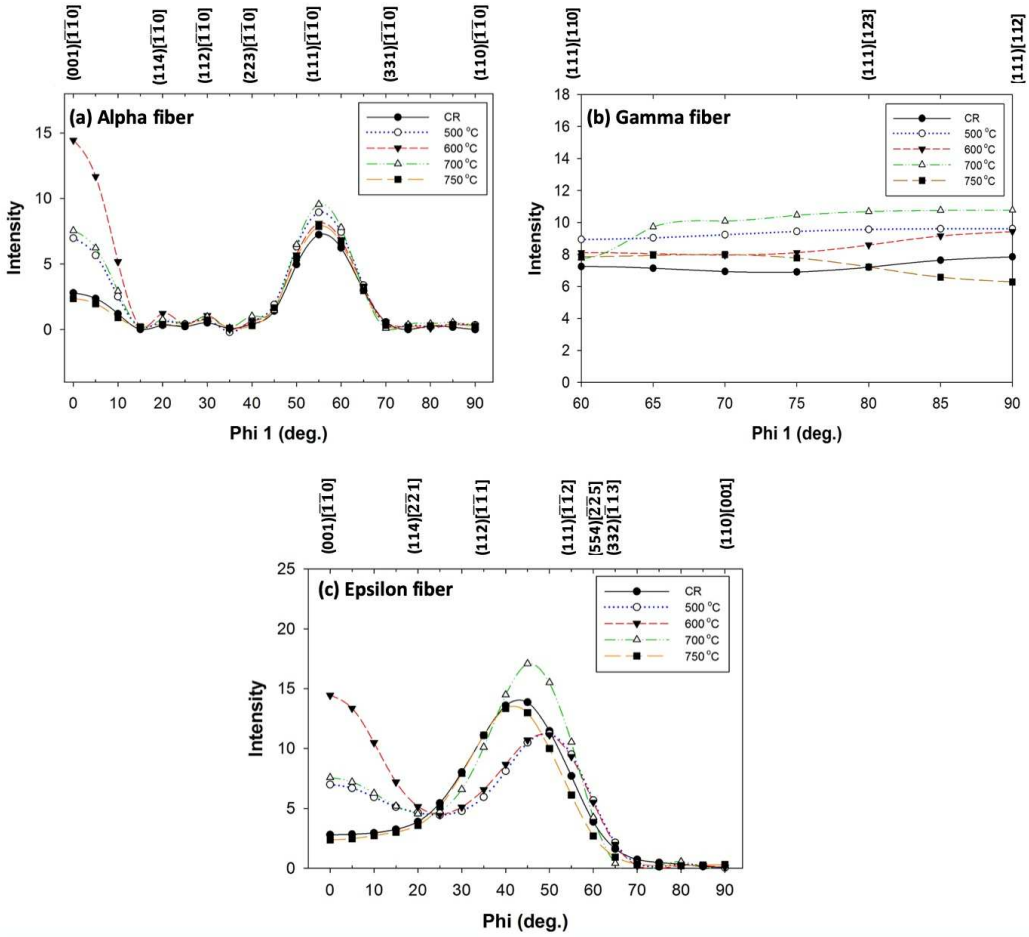

Fig. 16. Micro texture details of the samples. a) α-fiber, b) γ-fiber, c) ε-fiber for cold-rolled, 500°C-2h, 600°C-2h, 700°C-2h and 750°C-2h samples.

4. Summary and Conclusions

In order to clarify the microstructural evolution occurring in a 40Fe-50Co-10V alloy, the progress of static recrystallization in 86% cold-rolled sheets under various heat treatment conditions (temperatures 450–800 °C and durations 10–240 min) were studied utilizing especially the EBSD method. However, because the ordering reaction and austenite transformation are also concurrent, some observations on them had to be done. The most important findings are as follows:

1- Based on XRD patterns, the ordering process had occurred at 500 °C, being strongest at 600 °C after 2 hours and the intensity decreasing at higher temperatures. No long-range order reflection was observed after annealing at 750 °C for 2 hours.

2- Austenite phase particles could be detected by EBSD on ferrite grain boundaries after annealing for 2 hours at 550 °C and above. Their presence brought about the detection of the evolution of ferrite recrystallization complex without the phase distinction. Obviously, austenite transformation retarded the recrystallization and prevented effectively the grain growth.

3- The intense recovery in ferrite could be found by various techniques such as

analyses of Kernel Average Misorientation, Grain Orientation Spread and grain boundary misorientation distribution in addition to detection of sub-boundaries in EBSD grain boundary maps.

4- The kinetics of ferrite recrystallization was established. The start of ferrite recrystallization could be observed at 600 °C after 1 hour by the EBSD technique as small irregular-shaped ferrite grains surrounded by a high angle grain boundary and by analyzing the distributions of grain boundary misorientation. The determination of the recrystallized fraction is quite complex, however. The recrystallization kinetics seemed to be slow and only about 42% ferrite became recrystallized within 4 hours at 700 °C. The kinetics was much faster in the disordered state at 750 °C, but still sub-boundaries could be found after annealing for 4 hours in remnants of ferrite grains. It was estimated that the annealing duration of 10 hours would be needed for complete recrystallization at 750 °C.

5- Detailed observations on the evolution of grain boundary misorientations evidenced that the mechanism of static recrystallization is the continuous recrystallization. The texture components were almost unaltered during recrystallization, which supports the occurrence of this mechanism even in the disordered state.

Acknowledgments

MRK is grateful for financial support from the Iranian government for his research stay at the University of Oulu and for facilities and equipment provided by the University of Oulu for performing this study. LPK and JK acknowledge the support of the Academy of Finland for the “Genome of Steel” project #311934.

Authors Contributions

Mohammad Kamali performed the experiments, analyzed the data, prepared figures and wrote the main part of the draft manuscript. Pentti Karjalainen supervised the study, contributed to discussions by commenting, drawing conclusions and checking and revising the manuscript. Ali Mashreghi designed the experiments, supervised the project and commented the results. Saeed Hasani supervised the project, designed the experiments and draw conclusions. Vahid Javaheri participated preparation of figures and commenting and wrote the texture part. Jukka Komi contributed to discussions by commenting and general supervising.

Declarations of interest: none.

Data availability

The raw/processed data required to reproduce these findings cannot be shared at this time due to technical or time limitations.

References

[1] V.M. Zakharov, M.A. Libman, E.I. Estrin, On the role of atomic ordering in the formation of a high-coercivity state in iron-cobalt-vanadium alloys, Phys. Met. Metallogr. 113 (2012) 43–47. doi:10.1134/s0031918x12010152.

[2] S. Hasani, A. Shafyei, M. Shamanian, P. Behjati, H. Mostaan, T. Juuti, J.A. Szpunar, Correlation between magnetic properties and allotropic phase transition of Fe–Co–V alloy, Acta Metall. Sin. (English Lett.). 28 (2015) 1055–1058. doi:10.1007/s40195-015-0294-9.

[3] E. V. Artamonov, M.A. Libman, N.N. Rudanovskii, Magnetically hard materials for the motors of synchronous hysteresis electric motors, Steel Transl. 37 (2007) 547–551. doi:10.3103/S0967091207060186.

[4] B. Nabi, A.-L. Helbert, F. Brisset, R. Batonnet, G. André, T. Waeckerlé, T. Baudin, Effect of long range order on mechanical properties of partially recrystallized Fe49Co–2V alloy, Mater. Sci. Eng. A. 592 (2014) 70–76. doi:10.1016/j.msea.2013.10.093.

[5] T. Sourmail, Near equiatomic FeCo alloys: Constitution, mechanical and magnetic properties, Prog. Mater. Sci. 50 (2005) 816–880. doi:10.1016/j.pmatsci.2005.04.001.

[6] R.S. Sundar, S.C. Deevi, Soft magnetic FeCo alloys: alloy development, processing, and properties, Int. Mater. Rev. 50 (2005) 157–192. doi:10.1179/174328005X14339.

[7] V.I. Zel'dovich, Y.S. Samoylova, V.D. Sadovskiy, Morphological features of the formation of a gamma phase in deformed iron-cobalt-vanadium alloys, Phys. Met. Met. 42 (1976) 90–96.

[8] V.I. Zel'dovich, A.V. Doroshenko, Y.S. Samoylova, E.Z. Valiyev, S.G. Teploukhov, Ordering of the alpha phase in Vicalloy 1, Phys. Met. Met. 32 (1971) 61–69.

[9] S. Hasani, M. Shamanian, A. Shafyei, M. Nezakat, H. Mostaan, J.A. Szpunar, Effect of recrystallization and phase transitions on the mechanical properties of semihard magnetic FeCo-7.15V alloy during the thermomechanical process, Metall. Mater. Trans. A. 48 (2017) 1903–1909. doi:10.1007/s11661-017-3954-8.

[10] S. Hasani, A. Shafyei, M. Nezakat, H. Mostaan, P. Behjati, P. Sahu, The effect of the order-disorder transition on the electrical, magnetic and mechanical properties of Vicalloy I, Intermetallics. 81 (2017) 73–79. doi:10.1016/j.intermet.2017.02.027.

[11] S. Hasani, M. Shamanian, A. Shafyei, P. Behjati, J.A. Szpunar, Non-isothermal kinetic analysis on the phase transformations of Fe–Co–V alloy, Thermochim. Acta. 596 (2014) 89–97. doi:10.1016/j.tca.2014.09.020.

[12] F.J. Humphreys, M. Hatherly, Recrystallization of ordered materials, in: Recryst. Relat. Annealing Phenom., 2004: pp. 269–283.

[13] M.J. Marcinkowski, H. Chessin, Relationship between flow stress and atomic order in the FeCo alloy, Philos. Mag. 10 (1964) 837–859. doi:10.1080/14786436408225388.

[14] D.W. Clegg, R.A. Buckley, The disorder → order transformation in iron–cobalt-based alloys, Met. Sci. J. 7 (1973) 48–54. doi:10.1179/030634573790445541.

[15] S. Hasani, M. Shamanian, A. Shafyei, P. Behjati, H. Mostaan, P. Sahu, J.A. Szpunar, Electron microscopy study on grain boundary characterizations of Fe–Co–V alloy during annealing, Vacuum. 114 (2015) 1–5. doi:10.1016/j.vacuum.2014.12.025.

[16] R.S. Sundar, S.C. Deevi, Effect of heat-treatment on the room temperature ductility of an ordered intermetallic Fe-Co-V alloy, Mater. Sci. Eng. A. 369 (2004) 164–169. doi:10.1016/j.msea.2003.11.004.

[17] O. Mohanta, M. Ghosh, A. Mitra, A.K. Panda, Enhanced ferromagnetic ordering through nanocrystallization in cobalt incorporated FeSiBNb alloys, J. Phys. D. Appl. Phys. 42 (2009)

065007. doi:10.1088/0022-3727/42/6/065007.

[18] H. Mostaan, M. Shamanian, S. Hasani, J.A. Szpunar, Response of structural and magnetic properties of ultra-thin FeCo–V foils to high-energy beam welding processes, Int. J. Miner. Metall. Mater. 22 (2015) 1190–1198. doi:10.1007/s12613-015-1184-x.

[19] S. Hasani, M. Shamanian, A. Shafyei, P. Behjati, J.A. Szpunar, M. Fathi-moghaddam, Nano / sub-micron crystallization of Fe – Co – 7 . 15V alloy by thermo-mechanical process to improve magnetic properties, Mater. Sci. Eng. B. 190 (2014) 96–103. doi:10.1016/j.mseb.2014.09.013.

[20] B. Nabi, A.-L. Helbert, F. Brisset, G. André, T. Waeckerlé, T. Baudin, Effect of recrystallization and degree of order on the magnetic and mechanical properties of soft magnetic FeCo–2V alloy, Mater. Sci. Eng. A. 578 (2013) 215–221. doi:10.1016/j.msea.2013.04.066.

[21] W. Mao, G. Zhu, Y. Yu, Influence of order-disorder transition on the recrystallization behaviors of a cold rolled FeCo alloy, Z. Met. 91 (2000) 211–214.

[22] R.A. Buckley, Ordering and recrystallization in Fe-50Co-0.4%Cr, Met. Sci. 13 (1979) 67–72. doi:10.1179/msc.1979.13.2.67.

[23] R.A. Buckley, Microstructure and kinetics of the ordering transformation in iron–cobalt alloys, FeCo, FeCo–0.4%Cr, FeCo–2.5%V, Met. Sci. 9 (1975) 243–247. doi:10.1179/030634575790445080.

[24] A. Duckham, D.Z. Zhang, D. Liang, V. Luzin, R.C. Cammarata, R.L. Leheny, C.L. Chien, T.P. Weihs, Temperature dependent mechanical properties of ultra-fine grained FeCo–2V, Acta Mater. 51 (2003) 4083–4093. doi:10.1016/S1359-6454(03)00228-3.

[25] D.W. Clegg, R.A. Buckley, The disorder → order transformation in iron–cobalt-based alloys, Met. Sci. J. 7 (1973) 48–54. doi:10.1179/030634573790445541.

[26] G.B. Chon, K. Shinoda, S. Suzuki, B. Jeyadevan, Order-disorder transformation in Fe 50 Co 50 particles synthesized by polyol process, 51 (2010) 707–711. doi:10.2320/matertrans.M2009251.

[27] I. Ohnuma, H. Enoki, O. Ikeda, R. Kainuma, H. Ohtani, B. Sundman, K. Ishida, Phase equilibria in the Fe–Co binary system, Acta Mater. 50 (2002) 379–393. doi:10.1016/S1359-6454(01)00337-8.

[28] S. Hasani, M. Shamanian, A. Shafyei, P. Behjati, M. Nezakat, M. Fathi-Moghaddam, J.A. Szpunar, Influence of annealing treatment on micro/macro-texture and texture dependent magnetic properties in cold rolled FeCo–7.15V alloy, J. Magn. Magn. Mater. 378 (2015) 253–260. doi:10.1016/j.jmmm.2014.11.050.

[29] J.A. Ashby, H.M. Flower, R.D. Rawlings, Gamma phase in an Fe-Co-2%V alloy, Met. Sci. 11 (1977) 91–96. doi:10.1179/msc.1977.11.3.91.

[30] H.-P. Lin, D. Chen, J.-C. Kuo, Grain boundary evolution of cold-rolled fepd alloy during recrystallization at disordering temperature, Materials (Basel). 8 (2015) 3254–3267. doi:10.3390/ma8063254.

[31] S.I. Wright, M.M. Nowell, S.P. Lindeman, P.P. Camus, M. De Graef, M.A. Jackson, Introduction and comparison of new EBSD post-processing methodologies, Ultramicroscopy. 159 (2015) 81–94. doi:10.1016/j.ultramic.2015.08.001.

[32] W. Polkowski, P. Jóźwik, Z. Bojar, EBSD and X-ray diffraction study on the recrystallization of cold rolled Ni3Al based intermetallic alloy, J. Alloys Compd. 614 (2014) 226–233. doi:10.1016/j.jallcom.2014.06.106.

[33] J. Luo, R. Chu, W. Yu, Y. Chen, C. Zhang, Fine-grained processing and electron backscatter diffraction (EBSD) analysis of cold-rolled Inconel 617, J. Alloys Compd. 799 (2019) 302–313. doi:10.1016/j.jallcom.2019.05.193.

[34] A. Hadadzadeh, F. Mokdad, M.A. Wells, D.L. Chen, A new grain orientation spread approach to analyze the dynamic recrystallization behavior of a cast-homogenized Mg-Zn-Zr alloy using electron backscattered diffraction, Mater. Sci. Eng. A. 709 (2018) 285–289. doi:10.1016/j.msea.2017.10.062.

[35] N. Peranio, Y.J. Li, F. Roters, D. Raabe, Microstructure and texture evolution in dual-phase steels: Competition between recovery, recrystallization, and phase transformation, Mater. Sci. Eng. A. 527 (2010) 4161–4168. doi:10.1016/j.msea.2010.03.028.

[36] C.M. Sellars, Modelling microstructural development during hot rolling, Mater. Sci. Technol. 6 (1990) 1072–1081. doi:10.1179/mst.1990.6.11.1072.

[37] J. Huang, W.J. Poole, M. Militzer, Austenite formation during intercritical annealing, Metall. Mater. Trans. A. 35 (2004) 3363–3375. doi:10.1007/s11661-004-0173-x.

[38] N.Y. Zolotorevsky, V.V. Rybin, E.A. Ushanova, Analysis of grain misorientation distribution in polygonal ferrite of low-carbon steel, Mater. Charact. 122 (2016) 70–75. doi:10.1016/j.matchar.2016.10.022.

[39] L. Ryde, Application of EBSD to analysis of microstructures in commercial steels, Mater. Sci. Technol. 22 (2006) 1297–1306. doi:10.1179/174328406X130948.

[40] J. Hannula, D. Porter, A. Kaijalainen, M. Somani, J. Kömi, Mechanical properties of direct-quenched ultra-high-strength steel alloyed with molybdenum and niobium, Metals (Basel). 9 (2019) 350. doi:10.3390/met9030350.

[41] J. Wu, P.J. Wray, C.I. Garcia, M. Hua, A.J. Deardo, Image quality analysis: A new method of characterizing microstructures, ISIJ Int. 45 (2005) 254–262. doi:10.2355/isijinternational.45.254.

[42] C. Zheng, D. Raabe, Interaction between recrystallization and phase transformation during intercritical annealing in a cold-rolled dual-phase steel: A cellular automaton model, Acta Mater. 61 (2013) 5504–5517. doi:10.1016/j.actamat.2013.05.040.

[43] P. Moine, J.P. Eymery, P. Grosbras, The effects of short-range order and long-range order on the equilibrium configuration of superdislocations in Fe-Co : 2 at% V — Consequences on flow stress, Phys. Status Solidi. 46 (1971) 177–185. doi:10.1002/pssb.2220460115.

[44] S.V. Mehtonen, L.P. Karjalainen, D.A. Porter, Hot deformation behavior and microstructure evolution of a stabilized high-Cr ferritic stainless steel, Mater. Sci. Eng. A. 571 (2013) 1–12. doi:10.1016/j.msea.2013.01.077.

[45] R.H. Yu, S. Basu, Y. Zhang, A. Parvizi-Majidi, J.Q. Xiao, Pinning effect of the grain boundaries on magnetic domain wall in FeCo-based magnetic alloys, J. Appl. Phys. 85 (1999) 6655. doi:10.1063/1.370175.

[46] L. Ren, S. Basu, R.H. Yu, J.Q. Xiao, A. Parvizi-Majidi, Mechanical properties of Fe-Co soft magnets, J. Mater. Sci. 36 (2001) 1451–1457. doi:10.1023/A:1017588411888.

[47] R.K. Ray, J.J. Jonas, Transformation textures in steels, Int. Metal Rev. 35, (1990) 1–36.

[48] V. Javaheri, N. Khodaie, A. Kaijalainen, D. Porter, Effect of niobium and phase transformation temperature on the microstructure and texture of a novel 0.40% C thermomechanically processed steel, Mater. Charact. 142 (2018) 295–308. doi:10.1016/j.matchar.2018.05.056.

[49] D. Nyung, H. Nam, Recrystallization Textures of Metals and Alloys, in: Recent Dev. Study Recryst., InTech, 2013. doi:10.5772/54123.

Highlights:

- Recrystallization characteristics determined from multiple-analyses of EBSD data
- Austenite transformation starts at a lower temperature than recrystallization
- Ferrite recrystallization proceeds by intense recovery and continuous mechanism
- Ferrite recrystallization follows sigmoidal kinetics but is slow even at 750 °C

Declarations of interest: none.